Blackwell Publishing

Full-length article

Gene expression pattern in apoptotic QGY-7703 cells induced by homoharringtonine[1]

Wei JIN[2], Le-feng QU[3], Qin CHEN[4], Xin-zhong CHANG[2], Jiong WU[2], Zhi-min SHAO[2,5]

[2]*Breast Cancer Institute, Cancer Hospital, Department of Oncology, Shanghai Medical College, Institute of Biomedical Science, Fudan University, Shanghai 200032, China;* [3]*Department of Vascular Surgery and Institute of Vascular Surgery of PLA, Changhai Hospital, Shanghai 200433, China;* [4]*Shanghai Institute of Materia Medica, Chinese Academy of Sciences, Shanghai 201203, China*

Key words

Abstract

Aim: To classify the genes responsible for apoptosis in QGY-7703 cells induced by homoharringtonine (HHT). **Methods:** Apoptosis in QGY-7703 cells induced by HHT was demonstrated by DNA fragmentation and morphological observation. cDNA microarray technology was used to detect gene transcription, and the result of microarrays for genes was confirmed by RT-PCR. **Results:** Seventy-eight individual mRNA were identified and their transcription levels changed significantly. Those genes, of which 68% were upregulated and 32% were downregulated, were partially related to apoptosis. They were mostly oncogenes, tumor suppressors, enzymes, and kinases. **Conclusion:** HHT is a potential drug in the treatment of liver cancer. TGF-β, TNF, FAS, p38MAPK, and p53 apoptosis signaling pathways were activated during apoptosis in QGY-7703 cells. Such inducible genes may play important roles in apoptosis and deserve to be further studied.

Introduction

Liver cancer is most common in Asia. In China, about 100 000 patients die each year of primary liver cancer. To explore efficient drugs is very helpful for those patients to overcome liver cancer.

Homoharringtonine (HHT) is an alkaloid with antileukemia activity against a variety of acute myeloid leukemic cells. HHT can induce apoptosis in a variety of human myeloid leukemia cell lines[1,2]. In HL-60 cells, HHT induced apoptosis when the cells were exposed to 1×10^{-7} mol/L HHT for 4 h. DNA extracted from the treated cells showed a typical internucleosomal DNA degradation. This effect was in a concentration- and time-dependent manner. The results suggest that the antitumor mechanism of HHT is related to its activity to induce apoptosis[3]. HHT is an inhibitor of protein synthesis, its effect in a dose- and time-dependent manner. The extent of HHT-induced DNA formation correlates with the inhibition of DNA synthesis and loss of clonogenic survival[4]. However, so far, there have been no reports as to whether HHT can be used to treat liver cancer.

The purpose of this study is to explore the activity of HHT on liver cancer and to examine genes regulated by HHT treatment, so as to reveal the signal transduction pathway involved in HHT-induced apoptosis. cDNA microarrays were utilized to investigate changes of gene transcription. In all, 4 microarrays were screened and each array represented 14 218 human genes. The 78 genes characterized are mostly related to apoptosis, many of which are oncogenes, tumor suppressors, enzymes, and kinases. Moreover, a few of the identified genes are novel and may play important roles in apoptosis.

Materials and methods

Cell culture Human hepatoma QGY-7703 cells were cultured in RPMI-1640 medium containing 10% fetal bovine serum in a humid atmosphere with 5% CO_2 at 37 ℃. For the experiment, the QGY-7703 cells were incubated with 36 μmol·L^{-1} HHT (Beijing Union Pharmaceutical Factory, Beijing, China) or RPMI-1640 medium alone for 6, 24, and 48 h.
Detection of apoptotic DNA fragmentation Total cellular

DNA was extracted from the QGY-7703 cells according to the method described by Slin and Stafford with some slight modifications[5]. In brief, after washing in phosphate-buffered saline (PBS), the QGY-7703 cells were lysed overnight at 37 ºC in lysis buffer (10 mmol/L Tris-HCl, pH 8.0, 10 mmol/L edetic acid, 0.4% SDS, and 100 mg/L proteinase K). After completely dissolving, saturated phenol was added to the cell lysates and mixed entirely. The samples were then centrifuged for 5 min. Chloroform was added to the supernatant isolated from the previous step, mixed, and centrifuged. The supernatant was mixed with 2.5-fold volume of absolute ethanol and 0.2 mol/L NaCl for DNA precipitation. The DNA pellets were obtained by centrifugation at full speed for 10 min and then air-dried, dissolved in TE buffer containing 0.5 g/L RNase (Sigma Chemical Co, St Louis, MO, USA) at 37 ºC for 30 min. Electrophoresis was performed on 1.5% agarose gel. The DNA was visualized by UV illumination.

Morphological observation of apoptotic cells The QGY-7703 cells ($5×10^6$ cells, 2 mL/well) were seeded onto standard 6-well tissue culture plates and treated with HHT for 6, 24, and 48 h. The QGY-7703 cells on the plates were washed with PBS directly, then detached and centrifuged and washed with PBS. All cell samples were fixed in 4% paraformaldehyde and stained with 5 μg/mL Hoechst 33258 (Sigma Chemical Co, St Louis, MO, USA) for 15 min at room temperature; apoptosis was detected by fluorescence microscopy.

RNA isolation The total RNA from the QGY-7703 cells was extracted according to the original Chomczynski method with slight modifications[6]. The cells were collected and homogenized in Solution D containing 1% β-mercaptoethanol. After centrifugation, the supernatant was extracted with phenol:chloroform (1:1) twice and acidic phenol:chloroform (5:1) once. The RNA in the aqueous phase was precipitated by cold isopropanol and dissolved in deionized H_2O. Messenger RNA were purified using an Oligotex-dT mRNA Midi Kit (Qiagen, Pudong, Shanghai, China).

Construction of microarrays and probe preparation The microarrays were constructed according to Brown's method (http://cmgm.stanford.edu/pbrown/protocols/index.html). The 14 218 microarrays consisted of 14 218 full-length or partial cDNA representing novel, known, and control genes provided by United Gene Holdings (1111 Zhongshan Bei Er Road, Shanghai, China). The known genes were selected from the National Center for Biotechnology Information. Unigenes were set and cloned into a PBS plasmid vector. The control spots of non-human origin included the rice U2 RNA gene (8 spots), hepatitis C virus coat protein gene (8 spots), and spotting solution alone (32 spots). The cDNA

inserts were amplified by PCR using universal primers to the plasmid vector sequences. All PCR products were examined by agarose gel electrophoresis to ensure that the quality and the identity of the amplified clones were as expected. The PCR products were dissolved in the PCR buffer. The solution was spotted onto silylated slides (CEL Associates, Houston TX, USA) using a Cartesian PixSys 7500 motion control robot (Cartesian Technologies, Irvine, CA, USA) fitted with ChipMaker Micro-Spotting Technology (TeleChem International, Sunnyvale, CA, USA). Glass slides with spotted cDNA were then hydrated for 2 h in 70% humidity, dried for 0.5 h at room temperature, and then UV cross-linked (65 mj/cm). They were further processed at room temperature by soaking in 0.2% SDS for 10 min, subsequently in distilled H_2O for 10 min, and then in 0.2% sodium borohydride for 10 min. The slides were then dried and ready for hybridization.

The fluorescent cDNA probes were prepared through reverse transcription of the isolated mRNA and then purified according to the method described by Schena *et al*[7,8]. The mRNA samples from the control cells and treated cells were incubated with Cy5-dUTP (Amersham Pharmacia Biotech, Piscataway, NJ, USA). The 2 color probes were then mixed, precipitated with ethanol, and dissolved in 20 μL hybridization solution (5× SSC, 0.4% SDS, 50% formamide, and 5× Denhardt's solution).

Hybridization on microarrays The microarrays were prehybridized with hybridization solution containing 0.5 g/L denatured salmon sperm DNA at 42 ºC for 6 h. Fluorescent probe mixtures denatured at 95 ºC for 5 min were applied onto the prehybridized microarrays under cover glasses. After the microarrays were hybridized at 42 ºC for 15–17 h, they were stringently washed at 60 ºC for 10 min each in the solution of 2×SSC and 0.2% SDS, 0.1×SSC and 0.2% SDS, and 0.1× SSC, and then dried at room temperature.

Detection and analysis of microarrays The microarrays were scanned with a ScanArray 3000 (GSI Lumonics, Bellerica, MA, USA) at 2 wavelengths to detect emission from both Cy3 and Cy5. The acquired images were analyzed using ImaGene 3.0 software (BioDiscovery, Los Angeles, CA, USA). The intensities of each spot at the 2 wavelengths represent the quantity of Cy3-dUTP and Cy5-dUTP, respectively, hybridized to each spot. The ratio of Cy5 to Cy3 was computed for each location on each microarray. The overall intensities were normalized with a correction coefficient obtained using the ratio of 40 housekeeping genes (list of these genes is available at http://www.biodoor.com/). The genes were identified as differentially expressed if the ratio of Cy5/Cy3 was >2 or <0.5. To minimize artifacts arising from low

expression values, only genes with raw intensity values for both Cy3 and Cy5 of >800 counts were chosen for the differential analysis.

RT-PCR The total RNA was extracted from the cells with TRIzol reagent (Invitrogen Life Technologies, Carlsbad, CA, USA) and quantified by UV absorbance spectroscopy. The reverse transcription reaction was performed using the Superscript First-Strand Synthesis System (Invitrogen Life Technologies, USA) in a final volume of 20 μL containing 5 μg total RNA, 200 ng random hexamers, 1×reverse transcription buffer, 2.5 mmol/L MgCl$_2$, 1 mmol/L deoxynucleotide triphosphate mixture, 10 mmol/L DTT, RNase OUT recombinant ribonuclease inhibitor (Invitrogen Life Technologies, Carlsbad, CA, USA), 50 units Superscript reverse transcriptase (GIBCO-BRL, Gaithersburg, MD, USA), and diethyl-pyrocarbonate-treated water. After incubating at 42 °C for 50 min, the reverse transcription reaction was terminated by heating at 85 °C for 5 min. The newly synthesized cDNA was amplified by PCR. The reaction mixture contained 2 μL cDNA template, 1.5 mmol/L MgCl$_2$, 2.5 units Tag polymerase, and 0.5 μmol/L primer. The sequence for each primer used in this study was as follows:

TIEG primer (5'-ACTGCGGAGGAAAGAATGGA-3'; 5'-CTGGGAGGAGTGCTGGGAAC-3');

VDUP1 primer (5'-TTGCGGAGTGGCTAAAGTG-3'; 5'-TCATCTCAGAGCTGGTTCG-3'); protein phosphatase 1 (PPP1CA) primer (5'-ACTATTTGAGTATGGCGGTTTCC-3'; 5'-TGTTCTTGTCGGCGGGCTTG-3'); NFKBIA primer (5'-AAGACGAGGAGTACGAGCAGAT-3'; 5'-CAGCACCCAA-GGACACCAAA-3'); death-associated protein 6 (DAXX) primer (5'-GACCCAGACTCCGCATACC-3'; 5'-GCACTGA-CCTTTGCCTTTCC-3'); insulin-like growth factor binding protein 7 (IGFBP7) primer (5'-ATGCTGGAGAATATGAGT-GCCA-3'; 5'-CTGAAGCCTGTCCTTGGGAA-3'); inhibitor-of-differentiation (ID)3 primer (5'-GGAGCTTTTGCCACTGA-CTC-3'; 5'-TTCAGGCCACAAGTTCACAG-3'); and G3PDH primer (5'-ACCACAGTCCATGCCATCAC-3'; 5'-TCCACCA-CCCTGTTGCTGTA-3').

The amplication cycles were 94 °C for 3 min, then 33 cycles at 94 °C for 1 min, 58 °C for 1 min, 72 °C for 1.5 min, followed by 72 °C for 10 min. Aliquots of PCR product were electrophoresed on 1.5% agarose gels and visualized by ethidium bromide staining.

siRNA preparation and transfection The siRNA sequence targeting ID3 was 5'-AAGGAGCTTTTGCCACT-GACT-3'. The siRNA duplex was synthesized by Shanghai GeneChem (Zhangjiang, Shanghai). The cells in the exponential phase of growth were seeded in 6-well plates at a concentration of 5×10^5 cells/well. After incubation for 24 h,

the cells were transfected with siRNA (100 nmol/L) and Lipofectamine 2000 (Invitrogen Life Technologies, USA) according to the manufacturer's protocol. Silencing was examined 48 h after transfection. The control cells were treated with non-targeting siRNA.

Western blot analysis All cells on the plates were collected and detached from the plates. The cells were washed twice with PBS containing 1 mmol/L phenylmethylsulfonyl fluoride and lysed in cold TNT buffer [20 mmol/L Tris-HCl (pH 7.4), 200 mmol/L NaCl, 1% Triton X-100, 1 mmol/L phenylmethylsulfonyl fluoride, and 1% aprotinin] for 45 min with occasional rocking. The lysates were transferred to Eppendorf tubes and clarified by centrifugation at 12 000×*g* for 40 min at 4 °C. Identical amounts (50 μg of protein) of cell lysates were separated by 15% SDS-PAGE and transferred to the nitrocellulose. The membrane was incubated in blocking solution containing 5% powered milk in TBST [10 mmol/L Tris-HCl (pH 8.0), 150 mmol/L NaCl, and 0.1% Tween 20] at room temperature for 1 h. Then the membrane was immunoblotted with the specific antibodies against ID3 (Santa Cruz, Santa Cruz, CA, USA), cleaved caspase-3 (Cell Signaling Technology, Danvers, MA, USA) and antitubulin (Sigma-Aldrich, USA). Detection by enzyme-linked chemiluminescence was performed according to the manufacturer's protocol Amersham Pharmacia Biotech, USA).

Statistical analysis All of the data in Table 1 represent an average ratio of Cy5/Cy3 of 2 microarrays at each time point. Genes were identified as significantly expressed if the ratio of Cy5/Cy3 was >2 or <0.5.

Results

HHT induced apoptosis in QGY-7703 cells Apoptosis induced by HHT in the QGY-7703 cells was examined (Figure 1). DNA electrophoresis showed that the QGY-7703 cells presented the typical DNA ladder pattern of apoptosis after treatment with 36 μmol/L HHT for 24 and 48 h.

When stained with Hoechst-33258, the control cells that were not submitted to HHT treatment did not exhibit chromatin condensation (Figure 2A). By contrast, a dense and thin crown of nuclear coloration, typical of chromatin condensation, was observed in the HHT-treated cells at 24 h (Figure 2C). At the same time, some cells were detached from the plates, which was typical of chromatin condensation (Figure 2D). After treatment with HHT for 48 h, all of the cells detached from the plates, which was typical of chromatin condensation (Figure 2E). We found that although several nuclei still displayed a normal morphology, most of the cells
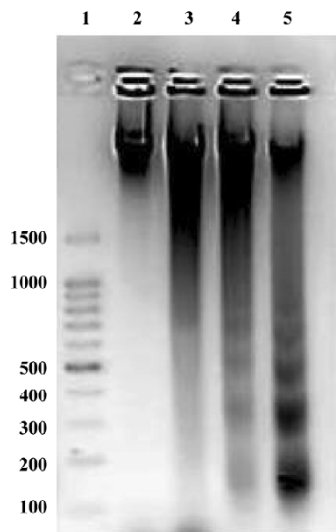
Figure 1. Patterns of DNA fragmentation during HHT induced apoptosis in QGY-7703 cells. 1) 100 bp DNA Ladder Marker; 2) untreated cells; 3) HHT 36 μmol/L, 6 h; 4) HHT 36 μmol/L, 24 h; 5) HHT 36 μmol/L, 48 h.

exhibited intense staining of condensed and fragmented chromatin. This evidence clearly showed that HHT induced apoptosis in the QGY-7703 cells.

cDNA microarray analysis In order to identify both early and late apoptosis-responsive genes, mRNA was isolated from the cells treated with HHT for 6 and 24 h, and subjected to microarrays for hybridization. RNA samples from cells treated with RPMI-1640 medium were used as the control. A total of 10 microarrays were screened. Two microarrays were screened for each parallel mRNA sample at each time point. The hybridization result was from all 10 microarrays, which were compiled and sorted on the basis of fold change compared to the control cells. The average ratio of the 2 microarrays screened at each time point was adopted. The hybridized signal of a desired gene displaying 2-fold or more changes was considered a significant change. Seventy eight of the 14 218 genes were identified by these criteria, 53 were upregulated, and 25 were downregulated at different time points (Table 1).

Confirmation of HHT-induced genes by RT-PCR To confirm the results obtained from the microarray hybridiza-tion, we used total RNA extracted from the cells and performed RT-PCR with 6 HHT-induced genes: ID3, TIEG, NFKBIA, VDUP1, PPP1CA, DAXX, and IGFBP7. The result showed that the expression patterns for the 6 genes correlated with the microarray results (Figure 3). The threshold we set for the inclusion of HHT-induced genes in the DNA chip analy-
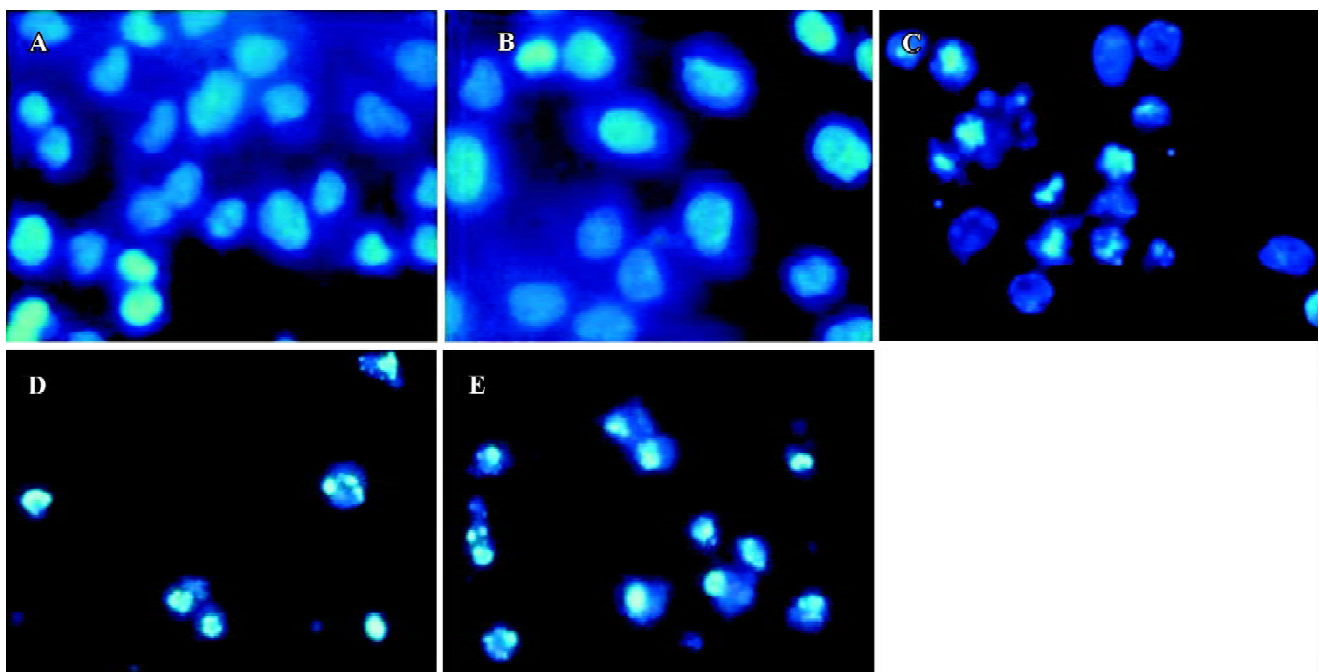
Figure 2. Photomicrograph of apoptotic changes in control (A) or treated with HHT for 6 h (B), 24 h on the plates (C), 24 h in suspension (D), 48 h in suspension (E). Cells were centrifuged and washed with PBS, fixed with 4% paraformaldehyde, and stained with Hoechst 33258 (5 μg/mL) for 15 min. The slides were then examined by fluorescence microscopy and photographed.

Table 1. List of differentially expressed genes responsive to HHT-induced apoptosis.

Symbol	GenBank_id	6 h	24 h	Definition
Apoptosis-related genes				
ID2*	NM_002166	1.76	8.47	inhibitor of DNA binding 2, dominant negative helix-loop-helix protein
ID3*	NM_002167	1.47	9.13	inhibitor of DNA binding 3, dominant negative helix-loop-helix protein
ACVRL1*	NM_000020	1.78	8.23	activin A receptor type II-like 1
TIEG*	NM_005655	6.15	10.39	TGFB inducible early growth response
EPHA2*	NM_004431	1.1	6.51	EPH receptor A2
ETS2*	NM_005239	1.1	6.26	v-ets erythroblastosis virus E26 oncogene homolog 2 (avian)
CYR61*	NM_001554	3.88	6.64	cysteine-rich, angiogenic inducer, 61
NFKBIA*	NM_020529	2.79	4.58	nuclear factor of kappa light polypeptide gene enhancer in B-cells inhibitor, alpha
TNFAIP3*	NM_006290	2.58	6.86	tumor necrosis factor, alpha-induced protein 3
BHLHB2	NM_003670	1.78	8.41	basic helix-loop-helix domain containing, class B, 2
VDUP1*	NM_006472	6.07	5.56	thioredoxin interacting protein, upregulated by 1,25-dihydroxyvitamin D-3
CYP1A1	NM_000499	1.68	7.29	cytochrome P450, subfamily I (aromatic compound-inducible), polypeptide 1
WEE1*	NM_003390	1.45	3.12	H.sapiens Wee1 gene.
RAD21*	NM_006265	0.4	0.8	RAD21 homolog (S. pombe)
DAXX*	NM_001350	1.06	0.45	death-associated protein 6
Oncogenes and tumor suppressors				
C-MYC*	NM_002467	2.02	4.95	C-MYC, oncogene
IGFBP3	NM_000598	1.27	7.22	insulin-like growth factor binding protein 3
PPP1CA*	NM_002708	3.32	3.15	protein phosphatase 1, catalytic subunit, alpha isoform
PIM2	NM_006875	1.43	2.02	pim-2 oncogene
RGS2	NM_002923	1.68	4.65	regulator of G-protein signalling 2, 24 kDa
ARHE	NM_005168	1.84	1.41	ras homolog gene family, member E
FOS*	NM_005252	2.74	6.01	v-fos FBJ murine osteosarcoma viral oncogene homolog
RAB13*	NM_002870	0.52	0.49	RAB13, member RAS oncogene family
IGFBP7*	NM_001553	0.55	0.21	insulin-like growth factor binding protein 7
Enzyme/kinases				
PDK2	NM_002611	1.61	8.85	pyruvate dehydrogenase kinase, isoenzyme 2
CLK2*	NM_001291	1.41	2.74	CDC-like kinase 2
ELL2	NM_012081	1.3	2.06	ELL-related RNA polymerase II, elongation factor
SNK	NM_006622	1.14	3.86	serum-inducible kinase
TK1*	NM_003258	1.67	3.92	thymidine kinase 1, soluble
CLK3	NM_001292	1.50	2.62	CDC-like kinase 3
PIK3R4*	NM_014602	2.56	10.27	phosphoinositide-3-kinase, regulatory subunit 4, p150
GADD34*	AK001361	1.02	4.99	protein phosphatase 1, regulatory (inhibitor) subunit 15A
PLAU	NM_002658	0.89	5.08	plasminogen activator, urokinase
MAP2K3*	NM_002756	1.51	5.42	mitogen-activated protein kinase kinase 3
ADAMTS1	NM_006988	2.46	2.93	a disintegrin-like and metalloprotease with thrombospondin type 1 motif, 1
ILK*	NM_004517	1.05	2.97	integrin-linked kinase
DHPS	NM_001930	1.31	2.34	deoxyhypusine synthase
DDX1*	NM_004939	0.56	0.4	DEAD/H (Asp-Glu-Ala-Asp/His) box polypeptide 1
DDX3*	NM_001356	0.3	0.24	DEAD/H (Asp-Glu-Ala-Asp/His) box polypeptide 3
DDX15*	NM_001358	0.47	0.23	DEAD/H (Asp-Glu-Ala-Asp/His) box polypeptide 15
MDH1	NM_005917	0.56	0.36	malate dehydrogenase 1, NAD (soluble)
P P	NM_021129	0.77	0.38	pyrophosphatase (inorganic)
O AT	NM_000274	0.35	0.39	ornithine aminotransferase (gyrate atrophy)
TARS	NM_003191	0.66	0.28	threonyl-tRNA synthetase
ALDH7A1	NM_001182	0.43	0.47	aldehyde dehydrogenase 7 family, member A1
RNASE3L	NM_013235	0.96	0.33	putative ribonuclease III
USP7	NM_003470	0.86	0.35	ubiquitin specific protease 7 (herpes virus-associated)

(Continue)

Symbol	GenBank_id	6 h	24 h	Definition
PRKDC	NM_006904	0.57	0.35	protein kinase, DNA-activated, catalytic polypeptide
ADPRT	NM_001618	0.54	0.24	ADP-ribosyltransferase (NAD+; poly (ADP-ribose) polymerase)
KYNU	NM_003937	0.58	0.45	kynureninase (L-kynurenine hydrolase)
Others				
NFIL3*	NM_005384	1.09	10.81	nuclear factor, interleukin 3 regulated
RBM4*	NM_002896	1.25	2.84	RNA binding motif protein 4
CD83	NM_004233	1.51	10.32	CD83 antigen (activated B lymphocytes, immunoglobulin superfamily)
COPEB	NM_001300	1.82	4.74	core promoter element binding protein
H4F2	M16707	1.3	5.22	H4 histone, family 2
CSRP1	NM_004078	1.33	3.19	cysteine and glycine-rich protein 1
SLC2A3	NM_006931	1.44	3.15	solute carrier family 2 (facilitated glucose transporter), member 3
TFAP2C	NM_003222	0.83	4.63	transcription factor AP-2 gamma (activating enhancer binding protein 2 gamma)
EIF5	NM_001969	1.28	1.59	eukaryotic translation initiation factor 5
PRCC	NM_005973	1.08	2.96	papillary renal cell carcinoma (translocation-associated)
CPSF4	NM_006693	1.43	3.35	cleavage and polyadenylation specific factor 4, 30 kDa
BRF1	NM_001519	1.25	3.22	BRF1 homolog, subunit of RNA polymerase III transcription initiation factor IIIB
BTG2	NM_006763	4.67	8.92	BTG family, member 2
CDH5	NM_001795	1.48	2.62	cadherin 5, type 2, VE-cadherin (vascular epithelium)
GIOT-2	NM_016264	1.04	2.12	GIOT-2 for gonadotropin inducible transcription repressor-2
H3F3B	NM_005324	1.22	2.41	H3 histone, family 3B (H3.3B)
GIF	NM_005142	0.91	2.92	gastric intrinsic factor (vitamin B synthesis)
DMBT1	NM_004406	1.23	3.44	deleted in malignant brain tumors 1
TOR1B	NM_014506	1.36	2.57	torsin family 1, member B (torsin B)
DDB2	NM_000107	1.01	2.28	damage-specific DNA binding protein 2, 48 kDa
HSPCA	NM_005348	0.79	0.48	heat shock 90 kDa protein 1, alpha
PSMA2	NM_002787	0.51	0.34	proteasome (prosome, macropain) subunit, alpha type, 2
IK	NM_006083	0.66	0.44	IK cytokine, down-regulator of HLA II
NCL	NM_005381	0.34	0.3	nucleolin
PSMD12	NM_002816	0.53	0.38	proteasome (prosome, macropain) 26S subunit, non-ATPase, 12
RCN1	NM_002901	0.44	0.34	reticulocalbin 1, EF-hand calcium binding domain
CCT4	NM_006430	0.83	0.39	chaperonin containing TCP1, subunit 4 (delta)
TMEFF1	NM_003692	0.56	0.52	transmembrane protein with EGF-like and two follistatin-like domains 1

Note: the gene labeled means the ones need explanation for the table.

sis is therefore valid in the 6 genes examined.

Reduction of ID3 expression by siRNA attenuates the HHT-induced activation of cleaved caspase-3 To determine the effect of siRNA on ID3 expression, cell lysates from the treated cells were analyzed by Western blotting. After treatment with HHT for 48 h, the expression of ID3 was inhibited by siRNA (Figure 4). Moreover, after the cells were treated with HHT for 48 h, cleaved caspase-3 could not be detected in ID3-targeting siRNA-treated cells (Figure 4).

Discussion

Most papers about HHT focus on antileukemia and apoptosis-inducing activity in leukemia cells[1–3]. Our experi-

ments showed that HHT could also induce apoptosis in human hepatoma QGY-7703 cells *in vitro*. In an attempt to identify genes in which expression changed significantly during HHT-induced apoptosis in the QGY-7703 cells, we utilized cDNA microarray technology to obtain an overall profile of gene expression.

Apoptosis-related genes Based on the data, our analysis was focused on those genes in which expression altered significantly during the process of cell apoptosis. Among those genes, we found that those capable of inducing apoptosis were upregulated, and the others protecting cells from apoptosis were downregulated.

Among the upregulated genes, ID2 and ID3 belong to a family of transcriptional modulators that are characterized
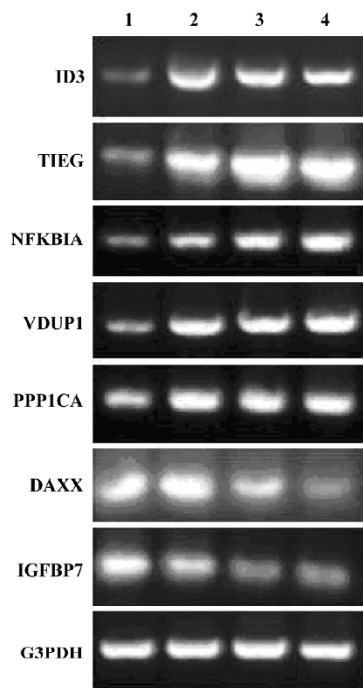
Figure 3. Effect of HHT on genes expression in apoptotic QGY-7703 cells. Total RNA was isolated from QGY-7703 cells treated with HHT for 6 h, 24 h, and 48 h. The reverse transcription reaction was performed using the Superscript First-Strand Synthesis System (Invitrogen Life Technologies, Inc). HHT-induced ID3, TIEG, NFKBIA, VDUP1, PPP1CA, DAXX, and IGFBP7 were amplified by PCR. G3PDH was used as an internal control. Aliquots of PCR product were electrophoresed on 1.5% agarose gels, and PCR fragments were visualized by ethidium bromide staining. 1) untreated cells; 2) HHT 36 μmol/L, 6 h; 3) HHT 36 μmol/L, 24 h; 4) HHT 36 μmol/L, 48 h.
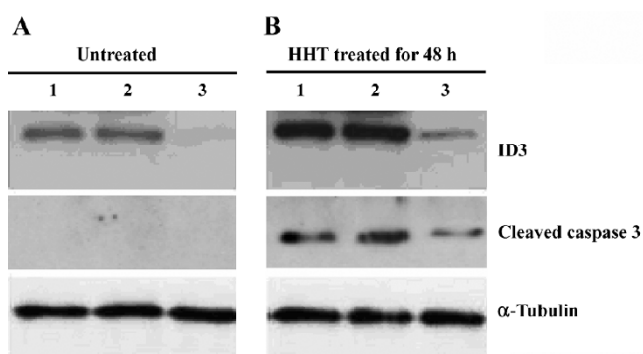
Figure 4. Reduction of ID3 expression by siRNAs attenuates the HHT-induced activation of cleaved caspase-3 in QGY-7703 cells. Cells were transfected with siRNAs targeting ID3 or with non-targetting siRNA for 48 h. Then transfected and untransfected cells were exposed to 36 μmo/L HHT for 48 h, cell lysates were prepared and performed Western-blot experiments. 1) control cells; 2) non-targetting siRNA cells; 3) siRNAs targeting ID3 cells. A: without HHT treatment; B: with HHT treatment for 48 h.

by a helix loop helix region. During development, ID2 is an inducible gene during serum and potassium deprivation-induced apoptosis of cerebellar granule neurons. Overexpression of ID2 induces neuronal cell death, both in high potassium and low potassium conditions. The inhibition of ID2 expression protects neurons from apoptosis[9]. ID2 may play a role in apoptosis-associated atrophy of skeletal muscles[10]. ID3 induces apoptosis through a caspase-2-dependent mechanism that does not require p53 and is not inhibited by bcl-2[11]. TIEG is an early growth response product induced by transforming growth factor-beta (TGF-β). Overexpression of TIEG mimics TGF-β action and plays a role in TGF-β-induced apoptosis in human osteoblast cells, pancreatic carcinoma cells, and epithelial and liver cancer cells[12–15]. ACVRL1 is type I cell-surface receptor recognized by the TGF-β superfamily[16]. The elevated expression levels of TIEG and ACVRL1 indicated that the TGF-β signaling pathways were initiated. CYR61 is cysteine-rich, angiogenic inducer 61, which can induce fibroblast apoptosis through its adhesion receptors, integrin $6\beta_1$, and the heparan sulfate proteoglycan syndecan-4, triggering the activation of the transcription-independent p53-activated Bax to render cytochrome c release and the activation of caspases-9 and -3[17]. TNFAIP3 represents TNF-α-induced protein 3, which encodes a protein that inhibits apoptosis[18]. NFKBIA is a nuclear factor for the kappa light chain gene enhancer in B-cells. It inhibits NF-κB activity by binding the rel domain of NF-κB components[19,20]. As known, NF-κB resists apoptosis. The upregulation of NFKBIA in our experiment would inhibit NF-κB activity and induce apoptosis. The upregulation of TNFAIP3 and NFKBIA indicated that the TNF signaling pathways were initiated. EphA2 is a target gene of the p53 family. P53 can bind to the promoter element of EphA2 and is responsive to wild-type p53, p73, and p63. EphA2 expression can result in an increase in apoptosis. The activated EphA2 may serve to impair anti-apoptotic signaling, disrupt focal adhesions, and thereby sensitize cells to pro-apoptotic stimuli[21]. ETS2 is a v-ets erythroblastosis virus E26 oncogene homolog 2. The overexpression of ETS2 results in apoptosis in trans-genic mice, cell lines, and in cells from subjects with Down syndrome. In all circumstances of ETS2 overexpression, the increased apoptosis correlated with increased p53 and alterations in downstream factors in the p53 pathway. The overexpression of ETS2 induces apoptosis that is dependent on p53 and involves the activation of caspase-3[22,23]. The upregulation of EphA2 and ETS2 indicated that the p53 signaling pathways were initiated. Vitamin D3 upregulated gene 1 (VDUP1)-mediated oxidative stress via suppressing the thioredoxin (TRX) function[24].

TRX has functions in defense against oxidative stress and control of growth. VDUP1 acts as an endogenous inhibitor of TRX by interacting with the catalytic active center of TRX to induce apoptosis and sensitize cells to oxidative stress-mediated apoptosis[25]. Wee1 is a well-known cell cycle regulator, which can interact with the Crk SH2 motif and accelerates apoptosis. Wee1-Crk complex signaling may be a novel apoptotic pathway[26].

Among the downregulated genes, DAXX is involved in apoptosis and transcriptional repression. It interacts with the death receptor FAS, promyelocytic leukemia protein (PML), and several transcriptional repressors. It may inhibit FAS and stress-mediated apoptosis by suppressing pro-apoptotic gene expression outside PML domains[27]. The inhibition of DAXX might trigger FAS signaling pathways. RAD21 is preferentially cleaved by caspases-3 and -7 to generate 2 major proteolytic products of 65 and 48 kDa. RAD21 is specifically proteolyzed by caspases into a subunit with a similar 65 kDa carboxyl-terminal product in cells undergoing apoptosis. Caspase proteolysis of RAD21 precedes apoptotic chromatin condensation and amplifies the cell death signal[28].

Oncogenes and tumor suppressors Among the upregulated genes, c-fos plays a causal role in clonal deletion of germinal center B cells[29]. The c-fos protein was found to induce apoptosis in 2 Syrian hamster embryo cell lines (sup+I and sup–II) and a human colorectal carcinoma cell line[30]. The catalytic subunit of protein phosphatase 1 (PPP1CA) regulates mitosis and is a putative tumor suppressor[31]. The induction of c-Myc may lead to apoptosis[32].

Among the downregulated genes IGFBP7 is a proto-oncogene. Rab13 is a Ras-associated small GTPase, which is presumed to function in vesicular traffic[33].

Enzyme/kinases Among the upregulated genes, CLK2 renders the cell hypersensitive to apoptosis triggered by oxidative stress or DNA replication block and gradually increases telomere length[34]. Thymidine kinase 1 (TK1) is a cell cycle regulatory gene involved in the G_1-S phase transition during cell cycle progression. The activation of TK1 may be critical to modulate radiation-induced cell death and cell cycle progression in irradiated K562 cells[35]. GADD34 is also known PPP1R15A, which is protein phosphatase 1, regulatory (inhibitor) subunit 15A. GADD34 is an apoptosis- and DNA damage-inducible gene[36,37]. Phosphoinositide-3-kinase regulatory subunit 4 (PIK3R4) is also called P150. It is reported that the expression of PIK3R4 correlates with tumor cell apoptosis[38], which can be cleaved by caspases both *in vitro* and *in vivo*[39]. MAP2K3 is mitogen-activated protein

kinase 3. The activation of p38MAPK is predominantly mediated by the 2 upstream MAPK kinases, MAP2K3 and MAP2K6. p38 is involved in apoptosis in many cell lines[40,41].

Among the downregulated genes, DDX1, DDX3, and DDX15 belong to the DEAD-box family. This family contains a large group of putative RNA helicases that mediate nucleoside triphosphate-dependent unwinding of double-stranded RNA. In their core region, DEAD-box proteins contain 9 conserved motifs, of which, asp-glu-ala-asp (DEAD), was adopted for the name of the whole family. They are implicated in a number of cellular processes involving the alteration of RNA secondary structures such as translation initiation, nuclear and mitochondrial splicing, and ribosome and spliceosome assembly. Based on their distribution patterns, some members of this family are believed to be involved in embryogenesis, spermatogenesis, and cellular growth and division.

Others NFIL3 is a nuclear factor and activates interleukin (IL)-3 gene expression. It binds to the regulatory sequence in the promoter region of adenovirus E4, gamma interferon, and IL-3 genes[42]. RNA binding motif protein 4 (RBM4), with a retroviral-type zinc finger, is a putative RNA recognition motif-type RNA-binding protein, which is similar to the D melanogaster lark RNA-binding protein[43].

To test whether these induced genes are related to HTT-induced apoptosis, we chose ID3 and tested its role in apoptosis. It is reported that the reduction of ID3 expression by siRNA abrogated the UVB-induced proteolytic activation of caspase-3[44]. We also found that reduction of ID3 expression by siRNA attenuated the HHT-induced activation of caspase-3 in the QGY-7703 cells, suggesting that HHT-induced apoptosis of QGY-7703 is at least in part due to the upregulation of ID3.

In conclusion, this was the first time that it was reported that HHT induced apoptosis of QGY-7703 cells *in vitro*. HHT is a potential drug against liver cancer. A variety of gene transcription has changed in apoptotic QGY-7703 cells; most genes with changed transcription were related to apoptosis, oncogenes and tumor suppressors, enzymes, and kinases. Our results demonstrated that TGF-β, TNF, FAS, p38MAPK, and p53 apoptosis signaling pathways were initiated. Some specific gene-encoding factors inducing apoptosis and tumor suppressors were upregulated. Oncogenes and some gene-encoding factors inhibiting apoptosis were downregulated. Other genes, such as DDX1, DDX3, DDX15, and RBM4 were induced significantly; they may play important roles in apoptosis signaling pathways and deserve to be further studied.

References

1 Lou YJ, Jin J, Xu WL, Tong XM. Homoharringtonine mediates myeloid cell apoptosis via upregulation of pro-apoptotic bax and inducing caspase-3-mediated cleavage of poly (ADP-ribose) polymerase (PARP). Am J Hematol 2004; 76: 199–204.

2 Jin W, Qu LF, Min P, Chen S, Li H, Lu H, *et al*. Identification of genes responsive to apoptosis in HL-60 cells. Acta Pharmacol Sin 2004; 25: 319–26.

3 Li L, Xia LJ, Jiang C, Han R. Induction of apoptosis by harringtonine and homoharringtonine in HL-60 cells. Acta Pharm Sin 1994; 29: 667–72.

4 Huang MT. Harringtonine, an inhibitor of initiation of protein biosynthesis. Mol Pharmacol 1975; 11: 511–9.

5 Darzynkiewicz Z, Bruno S, Del Bino G, Gorczyca W, Hotz MA, Lassota P, *et al*. Features of apoptotic cells measured by flow cytometry. Cytometry 1992; 13: 795–801.

6 Chomczynski P, Sacchi N. Single-step method of RNA isolation by acid guanidinium thiocyanate-phenol-chloroform extraction. Anal Biochem 1987; 162: 156–9.

7 Schena M, Shalon D, Davis RW, Brown PO. Quantitative monitoring of gene expression patterns with a complementary DNA microarray. Science 1995; 270: 567–70.

8 Schena M, Shalon D, Heller R, Chai A, Brown PO, Davis RW. Parallel human genome analysis: microarray-based expression monitoring of 1000 genes. Proc Natl Acad Sci USA 1996; 93: 10 614–9.

9 Gleichmann M, Buchheim G, El-Bizri H, Yokota Y, Klockgether T, Kugler S, *et al*. Identification of inhibitor-of-differentiation 2 (Id2) as a modulator of neuronal apoptosis. J Neurochem 2002; 80: 755–62.

10 Alway SE, Martyn JK, Ouyang J, Chaudhrai A, Murlasits ZS. Id2 expression during apoptosis and satellite cell activation in unloaded and loaded quail skeletal muscles. Am J Physiol Regul Integr Comp Physiol 2003; 284: 540–9.

11 Kee BL. Id3 induces growth arrest and caspase-2-dependent apoptosis in B lymphocyte progenitors. J Immunol 2005; 175: 4518–27.

12 Chalaux E, Lopez-Rovira T, Rosa JL, Pons G, Boxer LM, Bartrons R, *et al*. A zinc-finger transcription factor induced by TGF-beta promotes apoptotic cell death in epithelial Mv1Lu cells. FEBS Lett 1999; 457: 478–82.

13 Ribeiro A, Bronk SF, Roberts PJ, Urrutia R, Gores GJ. The transforming growth factor beta(1)-inducible transcription factor TIEG1, mediates apoptosis through oxidative stress. Hepatology 1999; 30: 1490–7.

14 Tachibana I, Imoto M, Adjei PN, Gores GJ, Subramaniam M, Spelsberg TC, *et al*. Overexpression of the TGF beta-regulated zinc finger encoding gene, TIEG, induces apoptosis in pancreatic epithelial cells. J Clin Invest 1997; 99: 2365–74.

15 Tau KR, Hefferan TE, Waters KM, Robinson JA, Subramaniam M, Riggs BL, *et al*. Estrogen regulation of a transforming growth factor-b inducible early gene that inhibits deoxyribonucleic acid synthesis in human osteoblasts. Endocrinology 1998; 139: 1346–53.

16 Attisano L, Carcamo J, Ventura F, Weis FM, Massague J, Wrana JL. Identification of human activin and TGF beta type I receptors that form heteromeric kinase complexes with type II

17 receptors. Cell 1993; 75: 671–80.

17 Todorovicç V, Chen CC, Hay N, Lau LF. The matrix protein CCN1 (CYR61) induces apoptosis in fibroblasts. J Cell Biol 2005; 171: 559–68.

18 Tewari M, Wolf FW, Seldin MF, O'Shea KS, Dixit VM, Turka LA. Lymphoid expression and regulation of A20, an inhibitor of programmed cell death. J Immunol 1995; 154: 1699–706.

19 Haskill S, Beg AA, Tompkins SM, Morris JS, Yurochko AD, Sampson-Johannes A, *et al*. Characterization of an immediate-early gene induced in adherent monocytes that encodes I kappa B-like activity. Cell 1991; 65: 1281–9.

20 Le Beau MM, Ito C, Cogswell P, Espinosa R 3rd, Fernald AA, Baldwin AS Jr. Chromosomal localization of the genes encoding the p50/p105 subunits of NF-kappa B (NFKB2) and the I kappa B/MAD-3 (NFKBI) inhibitor of NF-kappa B to 4q24 and 14q13, respectively. Genomics 1992; 14: 529–31.

21 Dohn M, Jiang J, Chen X. Receptor tyrosine kinase EphA2 is regulated by p53-family proteins and induces apoptosis. Oncogene 2001; 20: 6503–15.

22 Wolvetang EJ, Wilson TJ, Sanij E, Busciglio J, Hatzistavrou T, Seth A, *et al*. ETS2 overexpression in transgenic models and in Down syndrome predisposes to apoptosis via the p53 pathway. Human Mol Genet 2003; 12: 247–55.

23 Wolvetang EJ, Bradfield OM, Hatzistavrou T, Crack PJ, Busciglio J, Kola I, *et al*. Overexpression of the chromosome 21 transcription factor Ets2 induces neuronal apoptosis. Neurobiol Dis 2003; 14: 349–56.

24 Junn E, Han SH, Im JY, Yang Y, Cho EW, Um HD, *et al*. Vitamin D_3 up-regulated protein 1 mediates oxidative stress via suppressing the thioredoxin function. J Immunol 2000; 164: 6287–95.

25 Wang Y, De Keulenaer GW, Lee RT. Vitamin D_3-up-regulated protein-1 is a stress-responsive gene that regulates cardiomyocyte viability through interaction with thioredoxin. J Biol Chem 2002; 277: 26 496–500.

26 Smith JJ, Evans EK, Murakami M, Moyer MB, Moseley MA, Woude GV, *et al*. Wee1-regulated apoptosis mediated by the Crk adaptor protein in *Xenopus* egg extracts. J Cell Biol 2000; 151: 1391–400.

27 Chen LY, Chen JD. Daxx silencing sensitizes cells to multiple apoptotic pathways. Mol Cell Biol 2003; 23: 7108–21.

28 Chen F, Kamradt M, Mulcahy M, Byun Y, Xu HL, McKay MJ, *et al*. Caspase proteolysis of the cohesin component RAD21 promotes apoptosis. J Biol Chem 2002; 277: 16 775–81.

29 Inada K, , Phucharoen J, Hatano M, Sugimoto T, Moriya H, Tokuhisa T, *et al*. c-Fos induces apoptosis in germinal center B cells. J Immunol 1998; 161: 3853–61.

30 Preston GA, Lyon TT, Yin Y, Lang JE, Solomon G, Annab L, *et al*. Induction of apoptosis by c-Fos protein. Mol Cell Biol 1996; 16: 211–8.

31 Barker HM, Jones TA, da Cruz e Silva EF, Spurr NK, Sheer D, Cohen PT. Localization of the gene encoding a type I protein phosphatase catalytic subunit to human chromosome band 11q13. Genomics 1990; 7: 159–66.

32 Packham G, Cleveland JL. Ornithine decarboxylase is a mediator of c-myc-induced apoptosis. Mol Cell Biol 1994; 14: 5741–7.

33 Küppers R, Klein U, Schwering I, Distler V. Identification of Hodgkin and Reed-Sternberg cell-specific genes by gene expres-

sion profiling. J Clin Invest 2003; 111: 529–37.

34 Jiang N, Benard CY, Kebir H, Shoubridge EA, Hekimi S. Human CLK2 links cell cycle progression, apoptosis, and telomere length regulation. J Biol Chem 2003; 278: 21 678–84.

35 Jeong MH, Jin YH, Kang EY, Jo WS, Park HT, Lee JD, *et al*. The modulation of radiation-induced cell death by genistein in K562 cells: activation of thymidine kinase 1. Cell Res 2004; 14: 295–302.

36 Hollander MC, Zhan Q, Bae I, Fornace AJ Jr. Mammalian GADD34, an apoptosis- and DNA damage-inducible gene. J Biol Chem 1997; 272: 13 731–7.

37 Hollander MC, Poola-Kella S, Fornace AJ Jr. Gadd34 functional domains involved in growth suppression and apoptosis. Oncogene 2003; 22: 3827–32.

38 Chen G, Burger MM. p150 overexpression in gastric carcinoma: the association with p53, apoptosis and cell proliferation. Int J Cancer 2004; 112: 393–8.

39 Lane JD, Vergnolle MA, Woodman PG, Allan VJ. Apoptotic cleavage of cytoplasmic dynein intermediate chain and p150[Glued] stops dynein-dependent membrane motility. J Cell Biol 2001;

40 Tanaka N, Kamanaka M, Enslen H, Dong C, Wysk M, Davis RJ, *et al*. Differential involvement of p38 mitogen-activated protein kinase kinases MKK3 and MKK6 in T-cell apoptosis. EMBO Rep 2002; 3: 785–91.

41 Grethe S, Ares MP, Andersson T, Porn-Ares MI. p38 MAPK mediates TNF-induced apoptosis in endothelial cells via phosphorylation and downregulation of Bcl-x(L). Exp Cell Res 2004; 298: 632–42.

42 Zhang W, Zhang J, Kornuc M, Kwan K, Frank R, Nimer SD. Molecular cloning and characterization of NF-IL3A, a transcriptional activator of the human interleukin-3 promoter. Mol Cell Biol 1995; 15: 6055–63.

43 Jackson FR, Banfi S, Guffanti A, Rossi E. A novel zinc finger-containing RNA-binding protein conserved from fruitflies to humans. Genomics 1997; 41: 444–52.

44 Simbulan-Rosenthal CM, Daher A, Trabosh V, Chen WC, Gerstel D, Soeda E, *et al*. Id3 induces a caspase-3- and -9-dependent apoptosis and mediates UVB sensitization of HPV16 E6/7 immortalized human keratinocytes. Oncogene 2006; 25: 3649–60.

153: 1415–26.